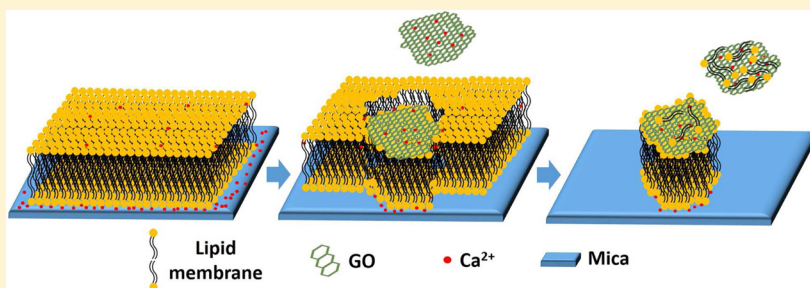


Morphology Change and Detachment of Lipid Bilayers from the Mica Substrate Driven by Graphene Oxide Sheets

Haozhi Lei,[†] Xuejiao Zhou,[‡] Haixia Wu,[‡] Yang Song,[†] Jun Hu,[†] Shouwu Guo,[‡] and Yi Zhang^{*,†}

[†]Key Laboratory of Interfacial Physics and Technology, Shanghai Institute of Applied Physics, Chinese Academy of Sciences, Shanghai 201800, China

[‡]Research Institute of Micro/Nano Science and Technology, Shanghai Jiao Tong University, Shanghai 200240, China



ABSTRACT: Understanding the interaction between graphene oxide (GO) and a lipid membrane is significant for exploring the biocompatibility and cytotoxicity of GO, which is the basis for utilizing GO in the fields of biosensors, bioimaging, drug delivery, antibacterials, and so on. In this article, we monitored the dynamic process of the morphology change and detachment of lipid bilayers on mica substrates prompted by GO sheets by *in situ* atomic force microscope (AFM) imaging. It was found that the bare lipid bilayer dramatically expanded in height and would be unstable and detachable from the mica substrates as induced by GO. The detached lipid molecules were found to bind to the GO surface. The results also imply that GO is likely to influence the height and stability of the supported lipid bilayers (SLBs) by adsorbing metal ions such as calcium ions that were used to stabilize the bilayer structures on the mica substrate. These findings illustrate a complicated effect of GO on the SLBs and should be helpful in future applications of GO in biotechnology.

INTRODUCTION

Graphene oxide (GO) is a widely used precursor for the mass production of graphene, which is an outstanding 2D inorganic material that has important applications in the fields of electronics,^{1,2} photonics,³ solar cells and capacitors,⁴ sensors,⁵ and so on.^{6,7} Because of good water solubility afforded by the enriched oxygen-containing groups, GO has also attracted numerous attention in biological science and has been found to have great potential in biosensors,^{8–10} drug delivery,¹¹ bioimaging^{12,13} and antibacterials.^{14,15} For biological applications, the biocompatibility and cytotoxicity of GO are critical issues.¹⁶ Unfortunately, until now researchers have not reached a consensus on the toxicity of GO in various biosystems.¹⁶ For example, Hu et al. found that GO paper has excellent antibacterial activity which can be used to inhibit the growth of bacteria, while it only slightly weakens the viability of a mammalian cell line A549.¹⁵ In contrast, Ruiz et al. reported that GO tends to increase microbial and mammalian cell proliferation dramatically.¹⁷ Similar arguments were also made with respect to the cytotoxicity of reduced GO (rGO) or pristine graphene.^{18–23}

Understanding how cells interact with GO will be helpful in considering the aforementioned arguments as well as for the practical applications of GO and graphene in biological systems. Previously, it was found that GO can induce the autophagy of

murine RAW 264.7 macrophages through the activation of membrane receptors of TLR4 and TLR9.²⁴ Liao et al. concluded that the hemolytic activity of both GO and graphene damaged skin fibroblasts and human erythrocytes.²¹ Generally, GO sheets may encounter a cell membrane first when it is presented in a cell culture medium, and the interaction between GO and cell membranes has become the focus of much research.^{14,17,25–29} Therefore, systems containing GO and liposomes or solid-supported lipid bilayers are widely investigated either theoretically or experimentally as convenient and direct models. For instance, Frost et al. reported that GO and lipid membranes can generate an altering multilayer structure through electrostatic interactions between GO and lipid headgroups.³⁰ In another case, Li et al. studied the GO/lipid membrane system at the air–water interface by using a Langmuir monolayer technique and found that GO interacts electrostatically with headgroups of lipids in different orientations.³¹ Liu's group systematically studied the interaction of GO with liposome and found that liposome can be absorbed on the side of GO;³² accordingly, a drug-delivery system was designed.^{33,34} Furukawa et al. reported that supported lipid

Received: February 27, 2014

Revised: April 15, 2014

Published: April 16, 2014

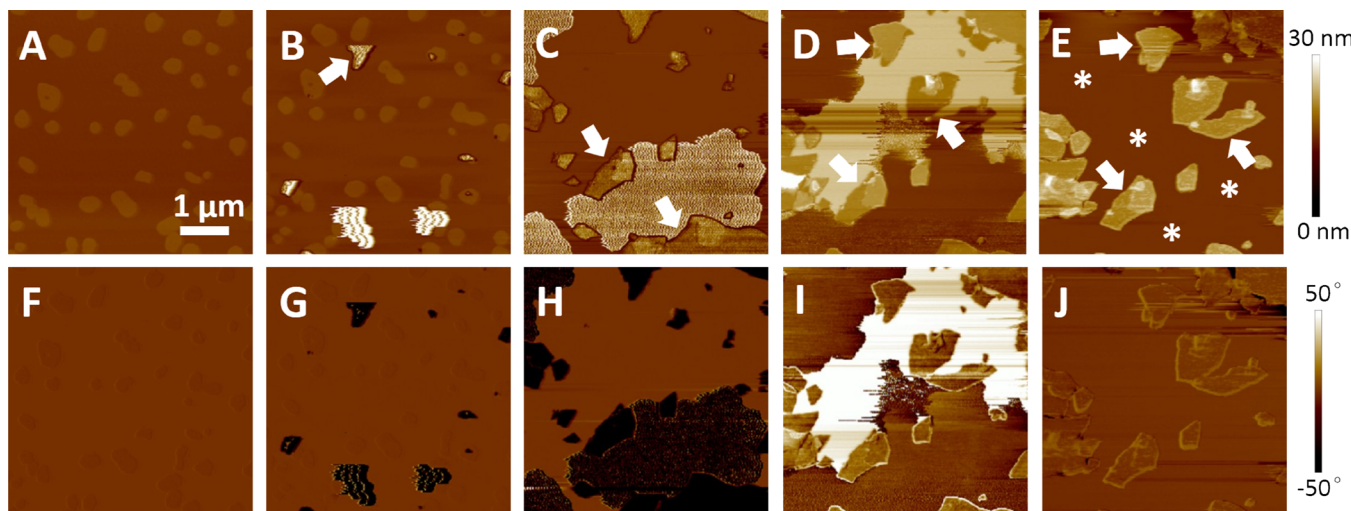


Figure 1. AFM height (A–E) and corresponding phase (F–J) images of the SLBs obtained at different times after adding GO to the AFM liquid cell. The SLBs were prepared with 10 mM CaCl₂, and the final GO concentration was 0.1 mg/mL. The arrows indicated the deposited GO sheets on the SLBs. (A, F) 0 min. (B, G) 5 min. There is noise at the GO positions in the images, which may be due to the fact that GO sheets were just deposited and had not settled stably on the SLBs. (C, H) 45 min. (D, I) 70 min. (E, J) 95 min. The asterisks indicate the SLB-detached area. The scale bar in A applies to all images. The Z scale bar in the upper right applies to images A–E, and the bar at the bottom right applies to images F–J.

bilayers (SLBs) cannot spread to the GO.³⁵ By using molecular simulation methods, researchers have revealed on the molecular level that electrostatic and hydrophobic forces are the main interactions between GO and lipid membranes.^{14,25–29}

Although much progress has been made, kinetic information on how the lipid membrane responds to GO remains to be illustrated. In this article, we presented a dynamic process showing the instability of lipid bilayers on mica substrates induced by GO nanosheets directly observed by atomic force microscopy (AFM), which is a versatile tool that allows dynamic high-resolution imaging of biological samples in physiological environments.^{36–41} It was found that the lipid bilayer exposed to water containing GO would expand in height and would be unstable and detach from the mica substrates. The detached lipid molecules were bonded to the GO surface. Our results also indicated that GO is likely to influence the height and stability of the SLBs by adsorbing metal ions such as Ca²⁺ or Mg²⁺ that were used to stabilize the bilayer structures on the mica substrate.⁴² These findings imply the complicated effects of GO on SLBs and should be helpful for exploring the applications of GO and SLBs further in biotechnology.⁴³

■ EXPERIMENTAL SECTION

Both dioleoylphosphatidylcholine (DOPC) and dipalmitoylphosphatidylcholine (DPPC) used in this study were purchased from Avanti Polar Lipids. Other reagents were purchased from Sigma. All of the reagents were used as received. Single-layer GO was produced from graphite powder with a modified Hummer's method and washed repeatedly with pure water.^{44–46}

Lipid vesicles were prepared following the procedures reported in the literatures.^{42,47} Briefly, DPPC and DOPC were mixed in a proportion of 1:1 (w/w) in chloroform to a final lipid concentration of 10 mg/mL, followed by evaporation of the solvent with nitrogen for more than 4 h. Then an aqueous solution of NaCl (20 mM) was added to the dried lipid mixture to a final lipid concentration of 1 mg/mL, which was suspended by ultrasonication for 4 h to form lipid vesicles.

A commercially available AFM instrument (Nanoscope 8, Bruker) equipped with a J scanner was used to study the evolution of the DPPC/DOPC bilayers on the mica substrate induced by GO. First, an aqueous solution of a divalent metal salt (CaCl₂ or MgCl₂) was added

to 20 μL of an as-prepared lipid vesicle solution to final salt and lipid vesicle concentrations of 10 mM and 0.1 mg/mL, respectively. Then the 20 μL lipid solution was injected into an AFM liquid cell in which mica was used as a sample substrate. It normally takes about 1 h for the lipid vesicles to transform into fully covered lipid bilayers on mica. The excess lipid vesicles were removed by pure water.^{47–50} After that, a drop of aqueous solution of single-layered GO was injected into the liquid cell to a final GO concentration of 0.1 mg/mL. AFM imaging of the SLBs was conducted in tapping mode with silicon nitride cantilevers (NP-S, Bruker) with a nominal force constant of 0.35 N/m. During AFM imaging, a minimal vertical load on the AFM tip was used.

■ RESULTS AND DISCUSSION

Figure 1 illustrates the changes in the SLBs (DPPC/DOPC 1:1) induced by adding the GO solution to the AFM liquid cell. The DPPC/DOPC SLBs prepared with 10 mM CaCl₂ showed a closely packed and domain-separated structure on mica (Figure 1A and 1F), which is consistent with that previously reported.⁴² From AFM images, it can be found that the flat DPPC islands were embedded in the homogeneous DOPC domains with a height of ~1 nm. Once the GO solution was introduced, the individual GO sheets started to deposit onto the SLBs (Figure 1B,G). Meanwhile, the SLBs around the GO sheets became unstable and detached gradually from the mica substrate. It was found that DPPC and DOPC domains detached from the mica substrate in a different order. Normally the DPPC domains disappeared first. As shown in Figure 1C–E, along with the deposition of more GO sheets, the area of the detached SLBs expanded. Finally, only the GO-covered SLBs remained on the mica substrate (Figure 1E). It is worth noting that the phase images, Figure 1H,I, displayed a distinct contrast, most probably due to the contamination of the AFM tip by the detached lipid molecules. This happens frequently in our experiments.

Strikingly, a change in the thickness of the SLBs was observed along with the deposition of GO sheets and the detachment of the SLBs from the mica substrate. Compared to the surrounding areas, GO-covered sites were found to be higher at the beginning (Figure 1C). However, they quickly

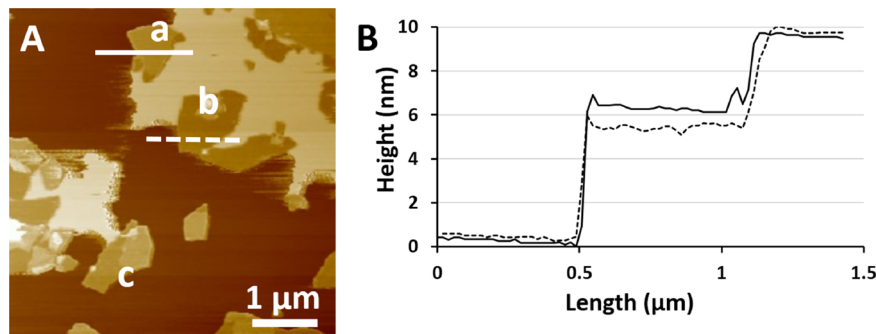


Figure 2. (A) AFM height image of the SLBs taken ~80 min after adding the GO solution to the liquid cell. (B) Section analysis of the 1.5 μm lines marked with (a) solid and (b) dashed lines in A.

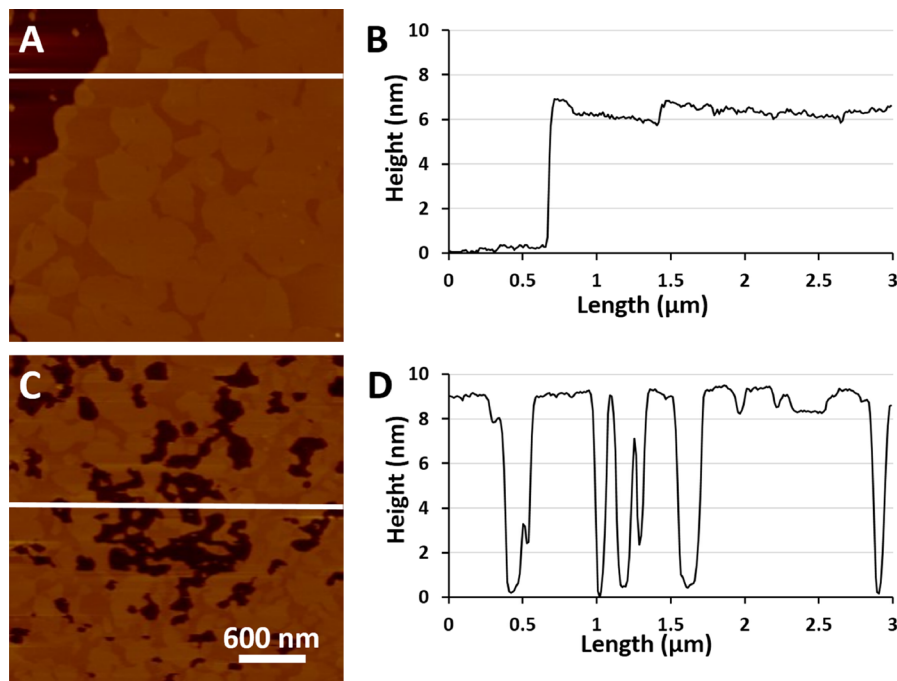


Figure 3. AFM height images (A, C) and corresponding section analyses (B, D) of DPPC/DOPC (1:1) bilayers on mica substrates prepared with (A, B) or without (C, D) 10 mM CaCl₂. In B, membrane thicknesses of about 5 and 6 nm were found, which corresponds to DOPC and DPPC domains, respectively. From D, membrane thicknesses of about 7.6 and 8.5 nm were found, which is corresponding to DOPC and DPPC domains, respectively. The final concentration of the lipid solution was decreased to 0.05 mg/mL to prepare non-fully-covered SLBs. The scale bar in C also applies to A.

decreased and became lower than the surrounding areas (Figures 1D), directly against the intuition that a GO-covered membrane should always be thicker than only a membrane. A detailed analysis of the membrane thickness in the later stage is shown in Figure 2. Clearly, the height of the bare SLBs was ~9 nm, while the height of the GO-covered sites is either ~6 nm (solid line in Figure 2B) or ~5 nm (dashed line in Figure 2B). The height difference of 1 nm at the GO-covered sites should be attributed to different domains of DPPC and DOPC on mica. However, the height difference between the GO-covered and bare SLBs means that the SLBs have two kinds of states after adding GO to the liquid cell.

It is interesting to determine why the thickness of SLBs varied after adding GO to the system. It is generally accepted that DPPC/DOPC bilayers have a height of 4–6 nm on mica substrate if the membrane is prepared in the presence of Ca²⁺.^{48,51} This is also confirmed in our experiments by AFM measurements of incompletely covered DPPC/DOPC bilayers

on mica (Figure 3A,B), which reveal average heights of 6.0 ± 0.2 nm (DPPC) and 5.0 ± 0.2 nm (DOPC), respectively. As we know, mica is negatively charged in water solution.^{52,53} The divalent cation Ca²⁺ in the system serves as a bridge between the mica surface and polar headgroups of the lipid molecules. Thus, it markedly reduces the thickness of the free water layer between mica and the lipid bilayers and stabilizes the bilayer structures on the substrate. After GO was added, the distribution of Ca²⁺ between mica and lipid membranes was changed. At the GO-covered locations, Ca²⁺ would still exist due to strong electrostatic adsorption of the GO on top. However, in the bare SLBs area, the Ca²⁺ under the bilayers would be attracted by GO that was either deposited nearby or in the solution through electrostatic interaction. As a result, the free water layer filled between the bilayers and mica substrate, thus increasing the height of the lipid bilayers.⁵⁴ This hypothesis was supported by our observation of a thickness of 8.5 ± 0.2 nm (DPPC) or 7.6 ± 0.2 nm (DOPC) on a mica

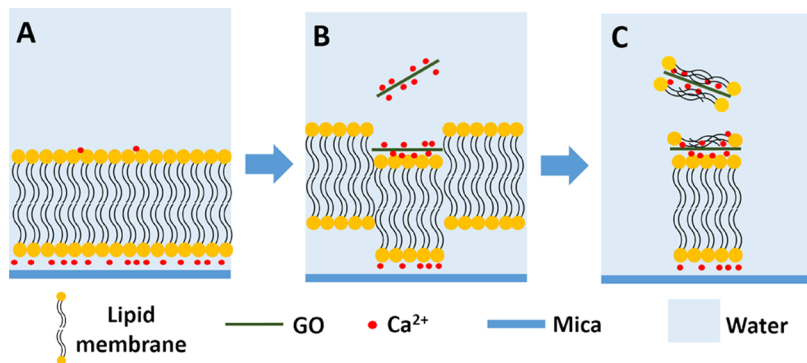


Figure 4. Schematic drawing illustrating how the thickness of the SLBs changes when GO is added. (A) Closely packed lipid bilayer that was stabilized with Ca²⁺ on a mica substrate. (B) Upon adding GO to the system, the height of the bilayer did not change very much at the GO-covered sites. However, at the bare SLBs, the Ca²⁺ under the bilayers would be attracted by GO that was either deposited nearby or was in the solution through electrostatic interaction. As a result, free water filled the space between the bilayers and mica substrate, thus increasing the apparent height of the lipid bilayers. (C) The bare lipid bilayer detached from the substrate so that only a GO-covered area remained.

substrate prepared without divalent cations in the solution (Figure 3C,D). On the basis of the above data, we suggest a possible explanation as to why the thickness of the SLBs changes in response to the presence of GO as shown in Figure 4.

To further study the role of Ca²⁺ in GO-induced instability and the detachment of SLBs from mica, we tried to use varied concentrations of CaCl₂ to prepare the SLBs. In one case, a DPPC/DOPC bilayer was prepared without Ca²⁺. In another case, a DPPC/DOPC bilayer was prepared with an extremely high concentration of CaCl₂, 1 M. AFM images indicate that in both cases the SLBs were stable and would not detach from the mica substrates after treatment with GO for 2 h (Figure 5). Moreover, very few GO sheets were found to deposit on the SLBs. It is understandable for the second case since there was enough Ca²⁺ to bridge the lipid and mica after being captured by GO. In the first case, because no divalent cation existed, the lipids should have formed 9 nm bilayers as shown in Figure 3C.

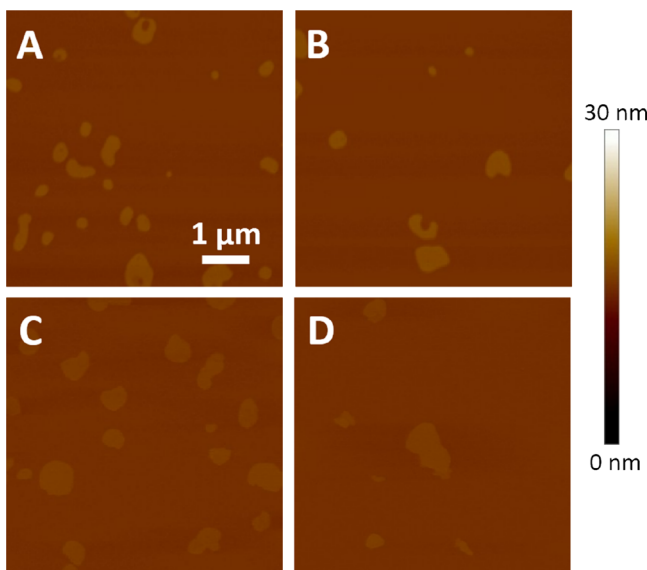


Figure 5. (A, B) AFM height images of DPPC/DOPC (1:1) SLBs prepared without CaCl₂ before (A) and after (B) adding GO for 2 h. (C, D) AFM height images of DPPC/DOPC (1:1) SLBs prepared with 1 M CaCl₂ before (C) and after (D) adding GO for 2 h. The scale bar in A applies to all images.

Thus, the addition of GO caused an undetectable change in the stability of the lipid bilayers. Our studies indicate that GO would induce membrane detachment from mica when CaCl₂ with a concentration in the range of 5 to 500 mM was used to prepare SLBs. It is worth noting that other divalent cations such as Mg²⁺ act similarly to Ca²⁺ with respect to the GO-induced instability of SLBs on mica (data not shown). In addition, a similar phenomenon was also observed on the membranes that were composed of lipid molecules with various DPPC/DOPC ratios. These results emphasize the important role of divalent cations in the GO-induced instability of SLBs.

It was found that the concentration of GO heavily affect the SLB detachment rate from the mica substrate. When GO solution was added to a final concentration of 0.4 mg/mL to the liquid cell, which was 4 times higher than the concentration used in Figures 1 and 5, the detachment of SLBs happened immediately and finished in half an hour (Figure 6A). On the

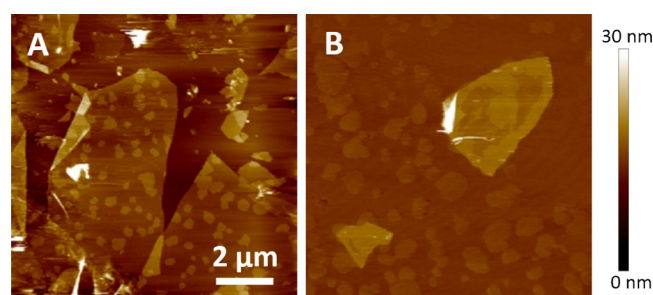


Figure 6. AFM height images indicating the DPPC/DOPC (1:1) SLBs after adding GO in varied concentrations. (A) Final GO concentration of 0.4 mg/mL. The image was taken 0.5 h after adding GO. (B) Final GO concentration of 0.01 mg/mL. The image was taken 2 h after adding GO. The scale bar in A applies to both images.

contrary, if the final concentration of GO was decreased to 0.01 mg/mL, then the destruction of SLBs dramatically slowed. For example, the SLBs remained on the mica substrate after treatment for 2 h (Figure 6B).

Previously, it has been reported that graphene or GO sheets would attract lipid molecules from membranes.^{33,34} Indeed, this was directly observed with AFM. Along with the disappearance of the DPPC and DOPC domains, lipid molecules tended to accumulate on the GO sheets (Figure 7A–C). In addition, the accumulation of lipid molecules on the GO sheets was also

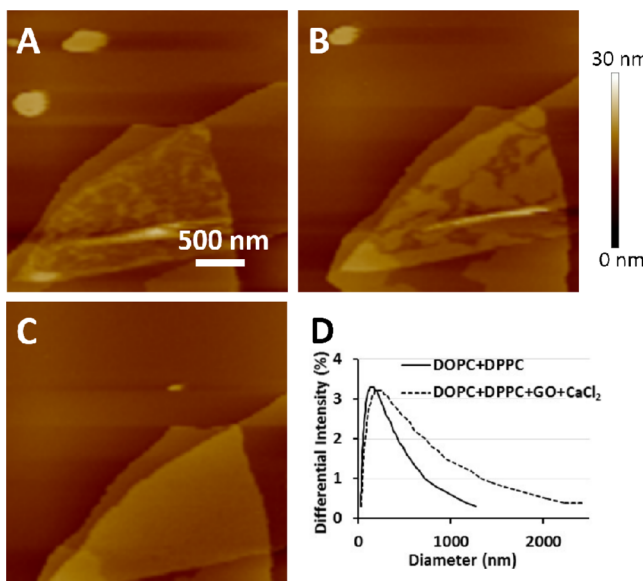


Figure 7. (A–C) AFM height images indicating the absorption of lipid molecules onto GO after adding it to the system for 20 (A), 60 (B), and 80 min (C), respectively. (D) Increase in the DOPC/DPPC vesicle size after adding GO to the system as detected by DLS.

detected with dynamic light scattering (DLS). When GO was gradually titrated into the DPPC/DOPC (1:1) liposome solution, the size of the complex increased gradually in a weight ratio of DPPC/DOPC/GO = 1:1:2 (w/w/w) (Figure 7D), which is consistent with previously studies.^{33,34}

CONCLUSIONS

We have shown a dynamic process illustrating the change in morphology and stability of lipid bilayers on mica substrates induced by GO sheets. It was found that the lipid bilayer changes its height when GO is introduced into the system, which would become unstable and detach later from the mica substrates. The results indicated that GO is likely to influence the SLBs by adsorbing metal ions such as calcium ions or magnesium ions that were previously used to stabilize the bilayer structures on the mica substrate. We believe that our findings have provided new insights into the interaction between GO and SLBs by emphasizing the role of divalent cations and should be helpful in upcoming explorations of the applications of GO in biotechnology.

AUTHOR INFORMATION

Corresponding Author

*E-mail: zhangyi@sinap.ac.cn.

Notes

The authors declare no competing financial interest.

ACKNOWLEDGMENTS

We are grateful for financial support from the National Basic Research Program of China (973 program, no. 2013CB932801) and the National Natural Science Foundation of China (nos. 11274334 and 11374205).

REFERENCES

- (1) Eda, G.; Fanchini, G.; Chhowalla, M. Large-area ultrathin films of reduced graphene oxide as a transparent and flexible electronic material. *Nat. Nanotechnol.* **2008**, *3*, 270–274.

(2) Gomez-Navarro, C.; Weitz, R. T.; Bittner, A. M.; Scolari, M.; Mews, A.; Burghard, M.; Kern, K. Electronic transport properties of individual chemically reduced graphene oxide sheets. *Nano Lett.* **2007**, *7*, 3499–3503.

(3) Blake, P.; Brimicombe, P. D.; Nair, R. R.; Booth, T. J.; Jiang, D.; Schedin, F.; Ponomarenko, L. A.; Morozov, S. V.; Gleeson, H. F.; Hill, E. W.; Geim, A. K.; Novoselov, K. S. Graphene-Based Liquid Crystal Device. *Nano Lett.* **2008**, *8*, 1704–1708.

(4) Wang, X.; Zhi, L. J.; Mullen, K. Transparent, Conductive Graphene Electrodes for Dye-Sensitized Solar Cells. *Nano Lett.* **2007**, *8*, 323–327.

(5) Zhou, M.; Zhai, Y. M.; Dong, S. J. Electrochemical Sensing and Biosensing Platform Based on Chemically Reduced Graphene Oxide. *Anal. Chem.* **2009**, *81*, S603–S613.

(6) Allen, M. J.; Tung, V. C.; Kaner, R. B. Honeycomb Carbon: A Review of Graphene. *Chem. Rev.* **2010**, *110*, 132–145.

(7) Geim, A. K.; Novoselov, K. S. The rise of graphene. *Nat. Mater.* **2007**, *6*, 183–191.

(8) Liu, S. J.; Wen, Q.; Tang, L. J.; Jiang, J. H. Phospholipid–Graphene Nanoassembly as a Fluorescence Biosensor for Sensitive Detection of Phospholipase D Activity. *Anal. Chem.* **2012**, *84*, 5944–5950.

(9) Ang, P. K.; Jaiswal, M.; Lim, C. H. Y. X.; Wang, Y.; Sankaran, J.; Li, A.; Lim, C. T.; Wohland, T.; Ozylmaz, B.; Loh, K. P. A Bioelectronic Platform Using a Graphene-Lipid Bilayer Interface. *ACS Nano* **2010**, *4*, 7387–7394.

(10) Hirtz, M.; Oikonomou, A.; Georgiou, T.; Fuchs, H.; Vijayaraghavan, A. Multiplexed biomimetic lipid membranes on graphene by dip-pen nanolithography. *Nat. Commun.* **2013**, *4*, 2591.

(11) Liu, J. Y.; Guo, S. J.; Han, L.; Wang, T. S.; Hong, W.; Liu, Y. Q.; Wang, E. K. Synthesis of phospholipid monolayer membrane functionalized graphene for drug delivery. *J. Mater. Chem.* **2012**, *22*, 20634–20640.

(12) Sun, X. M.; Liu, Z.; Welsher, K.; Robinson, J. T.; Goodwin, A.; Zaric, S.; Dai, H. J. Nano-graphene oxide for cellular imaging and drug delivery. *Nano Res.* **2008**, *1*, 203–212.

(13) Markovic, Z. M.; Ristic, B. Z.; Arsikin, K. M.; Klisic, D. G.; Harhaji-Trajkovic, L. M.; Todorovic-Markovic, B. M.; Kepic, D. P.; Kravic-Stevovic, T. K.; Jovanovic, S. P.; Milenkovic, M. M.; Milivojevic, D. D.; Bumbasirevic, V. Z.; Dramicanin, M. D.; Trajkovic, V. S. Graphene quantum dots as autophagy-inducing photodynamic agents. *Biomaterials* **2012**, *33*, 7084–7092.

(14) Tu, Y. S.; Lv, M.; Xiu, P.; Huynh, T.; Zhang, M.; Castelli, M.; Liu, Z. R.; Huang, Q.; Fan, C. H.; Fang, H. P.; Zhou, R. H. Destructive extraction of phospholipids from Escherichia coli membranes by graphene nanosheets. *Nat. Nanotechnol.* **2013**, *8*, 594–601.

(15) Hu, W. B.; Peng, C.; Luo, W. J.; Lv, M.; Li, X. M.; Li, D.; Huang, Q.; Fan, C. H. Graphene-Based Antibacterial Paper. *ACS Nano* **2010**, *4*, 4317–4323.

(16) Bianco, A. Graphene: Safe or Toxic? The Two Faces of the Medal. *Angew. Chem., Int. Ed.* **2013**, *52*, 4986–4997.

(17) Ruiz, O. N.; Fernando, K. A. S.; Wang, B. J.; Brown, N. A.; Luo, P. J. G.; McNamara, N. D.; Vangness, M.; Sun, Y. P.; Bunker, C. E. Graphene Oxide: A Nonspecific Enhancer of Cellular Growth. *ACS Nano* **2011**, *5*, 8100–8107.

(18) Rao, C. N. R.; Sood, A. K.; Subrahmanyam, K. S.; Govindaraj, A. Graphene: The New Two-Dimensional Nanomaterial. *Angew. Chem., Int. Ed.* **2009**, *48*, 7752–7777.

(19) Agarwal, S.; Zhou, X. Z.; Ye, F.; He, Q. Y.; Chen, G. C. K.; Soo, J.; Boey, F.; Zhang, H.; Chen, P. Interfacing Live Cells with Nanocarbon Substrates. *Langmuir* **2010**, *26*, 2244–2247.

(20) Chen, H.; Muller, M. B.; Gilmore, K. J.; Wallace, G. G.; Li, D. Mechanically strong, electrically conductive, and biocompatible graphene paper. *Adv. Mater.* **2008**, *20*, 3557–3561.

(21) Liao, K. H.; Lin, Y. S.; Macosko, C. W.; Haynes, C. L. Cytotoxicity of Graphene Oxide and Graphene in Human Erythrocytes and Skin Fibroblasts. *ACS Appl. Mater. Interfaces* **2011**, *3*, 2607–2615.

- (22) Park, S.; Mohanty, N.; Suk, J. W.; Nagaraja, A.; An, J. H.; Piner, R. D.; Cai, W. W.; Dreyer, D. R.; Berry, V.; Ruoff, R. S. Biocompatible, Robust Free-Standing Paper Composed of a TWEEN/Graphene Composite. *Adv. Mater.* **2010**, *22*, 1736–1740.
- (23) Li, Y. F.; Yuan, H. Y.; von dem Bussche, A.; Creighton, M.; Hurt, R. H.; Kane, A. B.; Gao, H. J. Graphene microsheets enter cells through spontaneous membrane penetration at edge asperities and corner sites. *Proc. Natl. Acad. Sci. U.S.A.* **2013**, *110*, 12295–12300.
- (24) Chen, G. Y.; Yang, H. J.; Lu, C. H.; Chao, Y. C.; Hwang, S. M.; Chen, C. L.; Lo, K. W.; Sung, L. Y.; Luo, W. Y.; Tuan, H. Y.; Hu, Y. C. Simultaneous induction of autophagy and toll-like receptor signaling pathways by graphene oxide. *Biomaterials* **2012**, *33*, 6559–6569.
- (25) Guo, R. H.; Mao, J.; Yan, L. T. Computer simulation of cell entry of graphene nanosheet. *Biomaterials* **2013**, *34*, 4296–4301.
- (26) Wang, J. L.; Wei, Y. J.; Shi, X. H.; Gao, H. J. Cellular entry of graphene nanosheets: the role of thickness, oxidation and surface adsorption. *RSC Adv.* **2013**, *3*, 15776–15782.
- (27) Radic, S.; Geitner, N. K.; Podila, R.; Kakinen, A.; Chen, P. Y.; Ke, P. C.; Ding, F. Competitive Binding of Natural Amphiphiles with Graphene Derivatives. *Sci. Rep.* **2013**, *3*, 2273.
- (28) Phan, A. D.; Hoang, T. X.; Phan, T. L.; Woods, L. M. Repulsive interactions of a lipid membrane with graphene in composite materials. *J. Chem. Phys.* **2013**, *139*, 1847031–1847035.
- (29) Titov, A. V.; Král, P.; Pearson, R. Sandwiched Graphene-Membrane Superstructures. *ACS Nano* **2009**, *4*, 229–234.
- (30) Frost, R.; Jonsson, G. E.; Chakarov, D.; Svedhem, S.; Kasemo, B. Graphene Oxide and Lipid Membranes: Interactions and Nanocomposite Structures. *Nano Lett.* **2012**, *12*, 3356–3362.
- (31) Li, S. H.; Stein, A. J.; Kruger, A.; Leblanc, R. M. Head Groups of Lipids Govern the Interaction and Orientation between Graphene Oxide and Lipids. *J. Phys. Chem. C* **2013**, *117*, 16150–16158.
- (32) Ip, A. C. F.; Liu, B. W.; Huang, P. J. J.; Liu, J. W. Oxidation Level-Dependent Zwitterionic Liposome Adsorption and Rupture by Graphene-based Materials and Light-Induced Content Release. *Small* **2013**, *9*, 1030–1035.
- (33) Wang, F.; Liu, B.; Ip, A. C.; Liu, J. Orthogonal adsorption onto nano-graphene oxide using different intermolecular forces for multiplexed delivery. *Adv. Mater.* **2013**, *25*, 4087–4092.
- (34) Wang, F.; Liu, J. W. Nanodiamond decorated liposomes as highly biocompatible delivery vehicles and a comparison with carbon nanotubes and graphene oxide. *Nanoscale* **2013**, *5*, 12375–12382.
- (35) Furukawa, K.; Hibino, H. Self-spreading of Supported Lipid Bilayer on SiO₂ Surface Bearing Graphene Oxide. *Chem. Lett.* **2012**, *41*, 1259–1261.
- (36) Hansma, P. K.; Elings, V. B.; Marti, O.; Bracker, C. E. Scanning Tunneling Microscopy and Atomic Force Microscopy - Application to Biology and Technology. *Science* **1988**, *242*, 209–216.
- (37) Czajkowsky, D. M.; Iwamoto, H.; Cover, T. L.; Shao, Z. F. The vacuolating toxin from Helicobacter pylori forms hexameric pores in lipid bilayers at low pH. *Proc. Natl. Acad. Sci. U.S.A.* **1999**, *96*, 2001–2006.
- (38) Fotiadis, D.; Scheuring, S.; Muller, S. A.; Engel, A.; Muller, D. J. Imaging and manipulation of biological structures with the AFM. *Micron* **2002**, *33*, 385–397.
- (39) Horber, J. K. H.; Miles, M. J. Scanning probe evolution in biology. *Science* **2003**, *302*, 1002–1005.
- (40) Lal, R.; Yu, L. Atomic-Force Microscopy of Cloned Nicotinic Acetylcholine-Receptor Expressed in Xenopus-Oocytes. *Proc. Natl. Acad. Sci. U.S.A.* **1993**, *90*, 7280–7284.
- (41) Pelling, A. E.; Li, Y. N.; Shi, W. Y.; Gimzewski, J. K. Nanoscale visualization and characterization of *Myxococcus xanthus* cells with atomic force microscopy. *Proc. Natl. Acad. Sci. U.S.A.* **2005**, *102*, 6484–6489.
- (42) Mineot-Leclercq, M. P.; Deleu, M.; Brasseur, R.; Duffrene, Y. F. Atomic force microscopy of supported lipid bilayers. *Nat. Protoc.* **2008**, *3*, 1654–1659.
- (43) Sackmann, E. Supported membranes: Scientific and practical applications. *Science* **1996**, *271*, 43–48.
- (44) He, H. Y.; Klinowski, J.; Forster, M.; Lerf, A. A new structural model for graphite oxide. *Chem. Phys. Lett.* **1998**, *287*, 53–56.
- (45) Zhang, J. L.; Yang, H. J.; Shen, G. X.; Cheng, P.; Zhang, J. Y.; Guo, S. W. Reduction of graphene oxide vial-ascorbic acid. *Chem. Commun.* **2010**, *46*, 1112–1114.
- (46) Hummers, W. S.; Offeman, R. E. Preparation of graphitic oxide. *J. Am. Chem. Soc.* **1958**, *80*, 1339–1339.
- (47) Giocondi, M. C.; Vié, V.; Lesniewska, E.; Milhiet, P. E.; Zinke-Allmang, M.; Le Grimellec, C. Phase Topology and Growth of Single Domains in Lipid Bilayers. *Langmuir* **2001**, *17*, 1653–1659.
- (48) Morandat, S.; Azouzi, S.; Beauvais, E.; Mastouri, A.; El Kirat, K. Atomic force microscopy of model lipid membranes. *Anal. Bioanal. Chem.* **2013**, *405*, 1445–1461.
- (49) Picas, L.; Milhiet, P. E.; Hernández-Borrell, J. Atomic force microscopy: A versatile tool to probe the physical and chemical properties of supported membranes at the nanoscale. *Chem. Phys. Lipids* **2012**, *165*, 845–860.
- (50) Andrecka, J.; Spillane, K. M.; Ortega-Arroyo, J.; Kukura, P. Direct Observation and Control of Supported Lipid Bilayer Formation with Interferometric Scattering Microscopy. *ACS Nano* **2013**, *7*, 10662–10670.
- (51) Leonenko, Z. V.; Finot, E.; Ma, H.; Dahms, T. E. S.; Cramb, D. T. Investigation of temperature-induced phase transitions in DOPC and DPPC phospholipid bilayers using temperature-controlled scanning force microscopy. *Biophys. J.* **2004**, *86*, 3783–3793.
- (52) Pashley, R. M.; Israelachvili, J. N. DLVO and hydration forces between mica surfaces in Mg²⁺, Ca²⁺, Sr²⁺, and Ba²⁺ chloride solutions. *J. Colloid Interface Sci.* **1984**, *97*, 446–455.
- (53) Mao, G. Z.; Tsao, Y. H.; Tirrell, M.; Davis, H. T.; Hessel, V.; Ringsdorf, H. Self-Assembly of Photopolymerizable Bolaform Amphiphile Monolayers and Multilayers. *Langmuir* **1993**, *9*, 3461–3470.
- (54) Giocondi, M.-C.; Yamamoto, D.; Lesniewska, E.; Milhiet, P.-E.; Ando, T.; Le Grimellec, C. Surface topography of membrane domains. *Biochim. Biophys. Acta, Biomembr.* **2010**, *1798*, 703–718.